Electronic Supplementary Material (ESI) for Nanoscale.
This journal is © The Royal Society of Chemistry 2022

Electronic Supplementary Information

Enhanced Nanocatalytic and Photoluminescent Efficiencies of Fe-O_4 Coordinated Carbon Dots via Core-Shell Synergistic Effect

Xiaoyan Wu,[a] Feng Yu,[b] Yifei Han,[c] Lei Jiang,[b] Zijian Li,[a]* Junfa Zhu,[d] Qian Xu,[d]* Antonio Claudio Tedesco,[be] Jiangwei Zhang[f] and Hong Bi[a]*

a. School of Materials Science and Engineering, Anhui University, Hefei 230601, China.

b. School of Chemistry and Chemical Engineering, Anhui University, Hefei 230601, China.

c. CAS Key Laboratory of Soft Matter Chemistry, Department of Polymer Science and Engineering, University of Science and Technology of China, Anhui 230026, China.

d. National Synchrotron Radiation Laboratory, University of Science and Technology of China, Hefei, Anhui 230029, China.

e. Department of Chemistry, Center of Nanotechnology and Tissue Engineering-Photobiology and Photomedicine Re-search Group, Faculty of Philosophy, Sciences and Letters of Ribeirão Preto, University of São Paulo, Ri-beirão Preto, São Paulo 14040-901, Brazil

f. College of Chemistry and Chemical Engineering, Inner Mongolia University, Hohhot 010021, China.

1. Experimental

1.1. Materials. All the chemicals used in the processes are commercially available and used without further purification. Ethylenediaminetetraacetic acid (EDTA), ferric chloride, 3,3′,5,5′-tetramethylbenzidine (TMB), glutathione (GSH), 5,5′-dithiobis (2-nitrobenzoic acid) (DTNB) and 5,5-dimethyl-1-pyrroline N-oxide (DMPO) were purchased from Aladdin Industrial Corporation (Shanghai, China). *o*-phenylenediamine (*o*-PD) was purchased from Shanghai Macklin Biochemical Co., Ltd. Glutaraldehyde (50%, *w*/*v*), paraformaldehyde and 2′,7′-dichlorofluorescein diacetate (H_2DCF-DA) were obtained from Sigma-Aldrich Fetal bovine serum (FBS), phosphate-buffered saline (PBS), Dulbecco's modified Eagle's medium (DMEM) (high glucose), penicillin/streptomycin and trypsin were purchased from Hyclone (Utah, USA), and calcein-AM/PI was purchased from BestBio (Shanghai, China). The LDH assay kit was obtained from Nanjing Jian Cheng BioChem Co. Ultra-pure water was used by all experiments from the Millipore system.

1.2. Instrumentation and Characterization. Morphological information was obtained by a transmission electron microscope (TEM, JEM-2100, JEOL, Tokyo, Japan). High-resolution transmission electron microscopy (HRTEM) measurements at different magnifications were conducted on the JEOL-F200 transmission electron microscope operating at 200 kV. Raman spectrum was recorded using a laser confocal micro-Raman spectroscopy (InVia-Reflex, Renishaw, London, Britain). Fourier transform infrared (FTIR) spectroscopy was collected using a Nexus 870 FTIR spectrometer. The X-ray photoelectron spectroscopy (XPS) was obtained with an

ESCALAB250 XPS using Al Kα radiation (1486.6 eV). Near Edge X-ray Absorption Fine Structure (NEXAFS) were carried out at the Catalysis and Surface Science Endstation at the BL11U beamline in the National Synchrotron Radiation Laboratory (NSRL) in Hefei, China. The X-ray absorption find structure spectra Fe K-edge were collected at 1W1B beamline of Beijing Synchrotron Radiation Facility (BSRF). Ultraviolet-visible (UV-Vis) spectra were measured using a UV-1800PC spectrophotometer (Shanghai meipuda instrument co., LTD, China). fluorescence spectra were obtained on a Hitachi FL-7100 (Hitachi high technologies corporation Tokyo Japan). The HORIBA FLSP920 system was used to obtain the absolute quantum yield (QY) in the calibration sphere. DMPO probes were used to evaluate the •OH generated by employing electron paramagnetic resonance (EPR, EMXnano, Bruker) at room temperature. The hydrodynamic diameters of EDTA-CDs and Fe@EDTA-CDs were measured in concentrated and dilute aqueous solutions using dynamic light scattering (DLS). Zeta potential analysis was performed on a Zetasizer analyzer (Nano ZS90, Malvern Instruments Ltd.). Quantitative analysis of Fe^{3+} was carried out by inductively coupled plasma mass spectrometry (ICP-MS) using the iCAP 7400 Duo system. Cyclic voltammetry (CV) and current time curve (i-t) tests were recorded on a CHI 660E electrochemical workstation in a three-electrode system at room temperature. Fluorescence microscopy images were recorded using Olympus IX-51 inverted fluorescence microscope (Olympus, Tokyo, Japan) and CLSM (Leica TCS SP8X).

1.3. Synthesis of CDs. The EDTA-CDs were prepared by the hydrothermal decomposition of ethylenediaminetetraacetic acid (EDTA) and *o*-phenylenediamine (*o*-

PD) dissolved in deionized water. Briefly, the mixture of EDTA (0.44 g), *o*-PD (0.20 g) and deionized water (30 mL) was transferred into 50 mL poly (tetrafluoroethylene)-lined autoclaves. After heating at 180 ℃ for 6 h, the solution was allowed to cool to room temperature naturally. The dark blue solution was filtered (0.22 μm) and dialyzed in regenerated cellulose dialysis tubing with MWCO 500-1000 for 48 h to remove unreacted EDTA-CDs and *o*-PD. Finally, the dialyzed solution was vacuum dried at -60 ℃ to collect a powder. As for the fabrication of the Fe@EDTA-CDs, 1 mg of EDTA-CDs was slowly added to 1 mL of different Fe^{3+} concentration aqueous solutions under ultrasonic irradiation at room temperature for 30 min. The products were dialyzed (MWCO 500-1000, Spectrum) against distilled water for 24 h to remove the free Fe^{3+} excess. The results showed that the fluorescence intensity reached the maximum value when the Fe^{3+} concentration was 1 mM. This particular complex component is selected here as the representative of our study.

1.4. Evaluation of •OH generation by MB decoloration experiment. degradation Methylene blue (MB) degradation was used to determine the generation of •OH through the Shimadzu UV-1800PC spectrophotometer. Specifically, Methylene blue (MB) (final working concentrations: 5 μg mL^{-1}) and Fe@EDTA-CDs were added to HAc/NaAc buffer (0.1 M, pH = 4). With the addition of H_2O_2 (final working concentrations: 1 mM), the MB was degraded, and the MB was degraded more at the same time under mild visible light irradiation (LED lamp, 400-500 nm, 100 mW cm^{-2}). The absorbance changes of MB at 665 nm were measured.

1.5. Evaluation of catalytic kinetic assay and photocatalytic activity. Before the

dynamic kinetic study, the optimal conditions of the catalytic oxidation of TMB with Fe@EDTA-CDs, such as reaction time and pH value, had been explored. The Michaelis-Menten constants, including the maximum velocity (v_{max}), Michaelis–Menten constant (K_m), and turnover number (TON), were calculated based on the Michaelis-Menten saturation curve. For each H_2O_2 concentration, the initial reaction rates (v_0) of the oxidation of TMB were calculated from the absorbance variation using the Beer-Lambert Law (Equation (S1)) (with an ε of 39,000 M^{-1} cm^{-1} for oxTMB, which indicates the oxTMB concentration and l for the length of the solution in the light path). The reaction rates were then plotted against their corresponding H_2O_2 concentration and then fitted with a linear double-reciprocal plot (Lineweaver-Burk plot, Equation (S2)) to determine v_{max} and K_m. Furthermore, TON was calculated according to equation (S3)

$$A = \varepsilon lc \quad (S1)$$

$$\frac{1}{v} = \frac{K_m}{v_{max}[S]} + \frac{1}{v_{max}} \quad (S2)$$

$$\mathrm{TON} = \frac{v_{max}}{[\mathrm{E}_0]} \quad (S3)$$

Where v represents the initial reaction velocity, K_m represents the Michaelis constant, [S] is the substrate concentration, and v_{max} is the maximal reaction velocity. $[\mathrm{E}_0]$ is the mole concentration of metal in the whole nanomaterials.

The photocatalytic activity of the Fe@EDTA-CDs was assessed under visible light irradiation. A visible light (LED lamp, 400-500 nm, 100 mW cm^{-2}) was used as the light source and placed 50 mm from the reaction position. Typically, the Fe@EDTA-CDs (20 μg mL^{-1}) were added into the acetate buffer solution (0.1 M, pH = 4), containing 1 mM TMB and H_2O_2. The catalytic activity change of Fe@EDTA-CDs

during photocatalysis was measured via the detection of the absorbance at 652 nm on a UV-1800 PC spectrophotometer.

1.6. Electrochemical Characterization: The Cyclic voltammetry and transient photocurrent were conducted at CHI 660 Electrochemical workstation in a three-electrode system using platinum foil, the Fe@EDTA-CDs, and saturated calomel electrode (SCE) as the counter, working and reference electrodes, respectively. Solution of HAc/NaAc buffer (0.1 M, pH = 4) was used as the electrolyte and a LED light was utilized as the visible light source. The photocurrent signal was observed at a constant potential of + 0.5 V versus SCE.

1.7 For the simplified molecular model of Fe@EDTA-CDs. Geometry optimization: For complex Fe@EDTA-CDs, it was optimized by using B3LYP (unrestricted) as exchange functional. All non-metallic atoms (including C, H, O and N) were described via utilizing 6-31G(d) as basis set, while Los Alamos effective core potential was employed to depict Fe^{3+}.

TDDFT calculation: To simulate UV-vis spectrum, PBE1PBE was selected as the exchange functional. For Fe^{3+} and non-metallic elements, they were described by the same methods that were exploited in the structural optimization step.

1.8. *In Vitro* Cytotoxicity Assay. The HepG2 cells, SY5Y cells and HUVEC cells were adopted to evaluate the cytotoxicity of EDTA-CDs and Fe@EDTA-CDs through Cell Counting Kit-8. Briefly, the HepG2 cells were inoculated at 1×10^4 cells per well in 96-well cell culture plates with 10% (*v*/*v*) fetal bovine serum and 1% (*v*/*v*) penicillin-streptomycin in DMEM and then incubated in a humidified atmosphere at 37 °C

containing 5% CO_2 for 24 h. The EDTA-CDs and Fe@EDTA-CDs were then placed under UV light and sterilized for 24 h. The EDTA-CDs and Fe@EDTA-CDs were then dispersed in H_2O and added to each well at increasing concentrations (0, 10, 20, 40, 60, 80, and 100 μg mL^{-1}) to incubate with the cells for 24 h. Then 10 μL of Cell Counting Kit-8 was added to each well and left for 4 h in the dark. Finally, the optical density (OD) was recorded at 450 nm using an enzyme marker (CMAX PLUS, SpectraMax® Absorbance Reader). The experiments were repeated three times.

The extracellular lactate dehydrogenase release level (LDH) was used to indicate membrane permeability and cytotoxicity. In the LDH assay, the HepG2 cells were inoculated in 96-well cell culture plates at a density of 1×10^4 cells per well for 24 h. Then different concentrations of the EDTA-CDs and Fe@EDTA-CDs were added to the designed wells and co-incubated with the cells for 24 h. An enzyme marker measured the LDH release in each sample with 630 nm as the reference wavelength and 450 nm as the detection wavelength. The results of the LDH assay was expressed as mean absorbance values compared to the untreated control cells. The experiment was repeated three times, and $p < 0.05$ was considered significant.

The mouse red blood cells (RBCs) were obtained by removing serum from the blood by centrifugation and washing. Then RBCs were suspended in normal saline was mixed with an equal volume of CDs solution at a final CDs concentration of 10, 20, 40, 60, 80, or 100 μg mL^{-1}. RBCs in normal saline and 1% Triton X-100 solution were set as negative and positive controls, respectively. After the mixtures were incubated at 37 °C for 2 h and centrifugated for 5 min, the absorbance at 450 nm of these

supernatants was measured using a microplate reader. The hemolysis percentage was calculated using the following formula:

$$\text{Hemolysis Rate (\%)} = \left(\frac{A_{sample} - A_{PBS}}{A_{blank} - A_{PBS}}\right) \times 100\% \quad \text{(S4)}$$

Among them, A_{sample}, A_{PBS}, and A_{blank} represent the absorbance of the experimental group, negative control, and positive control, respectively.

1.9. Cellular imaging. HepG2 cells were first cultured at 37 ºC overnight. In the colocalization experiment, HepG2 cells were first incubated with EDTA-CDs and Fe@EDTA-CDs (80 μg mL^{-1}) at 37 ºC for 2 h, and the commercial dyes of Lyso-Tracker Green (50 nM) for 30 min. Then, the cells were washed with PBS solution three times and imaged. Fluorescent imaging experiments were carried out in living cells on CLSM (CLSM, Leica TCS SP8X) with the λ_{ex} at 488 and 561 nm. The colocalization experiments were repeated three times.

1.10. Bio-TEM. The 0.1 M cacodylate buffer containing glutaraldehyde (2.5%, *v*/*v*) solution was used to fix the seeded cells and then added 1% osmium tetroxide (*w*/*v*). After dehydration with methanol, the cells were infiltrated and finally implanted in Epoxy resin. The ultrathin section was counter-stained with 4% uranyl acetate (*w*/*v*), lead citrate, and finally monitored under the electron microscope (JEM-2100, JEOL, Tokyo, Japan).

1.11. Detection of the reactive oxygen species (ROS). HepG2 cells were incubated using 6-well plates. Then, 2 mL of 80 μg mL^{-1} Fe@EDTA-CDs (100 μM H_2O_2 or not) was added to the cells and incubated for 6 h. As for laser irradiation groups, all of the treatment was similar to that above and irradiated by a LED light for 12 min. Then,

DCFH-DA (10 μM) was dropped in. After 15 min, fluorescence imaging was performed.

1.12. Live/Dead Cell Staining Assay. The calcein-AM and propidium iodide (PI) was used to evaluate the live and dead cells. HepG2 cells were seeded in a six-well plate with a density of 1.0×10^5 cells per well and incubated with EDTA-CDs and Fe@EDTA-CDs at the same concentration (80 μg mL^{-1}). As for laser irradiation groups, all treatment was similar to that above and irradiated by a LED light for 12 min. After all the treatment, 4T1 cells were stained with calcein-AM (2 μM) and PI (4 μM) and then analyzed by fluorescence microscopy.

1.13. Growth Inhibition Effect of Fe@EDTA-CDs on MCs. First, 0.45 g poly HEMA was added to 30 mL of a 95% ethanol solution and kept stirring at 37 °C for 24 h. Then, 5 mL of a completely dissolved poly HEMA mixture was added to each cell culture flask, which was kept in an oven for 24 h at 37 °C to form a thin film layer on the bottom of the cell culture flask. Third, coated flasks were exposed under UV light for 12 h to sterilize. To form HepG2 MCs, 5×10^5 HepG2 cells was coincubated with 5 mL of fresh DMEM, were placed in the coated flasks. The cells were incubated under a humidified atmosphere containing 5% CO_2 at 37 °C, and the DMEM was replaced every other day. HepG2 MCs with diameters of 300-400 μm were formed spontaneously after 7 days. A fluorescence microscope observed the cytotoxicity of Fe@EDTA-CDs and HepG2 MCs. A total of 30 - 40 MCs with diameters of 300-400 μm were transferred to a six-well cell culture plate coated with poly HEMA and then co-incubated with DMEM, H_2O_2 and Fe@EDTA-CDs + H_2O_2 for 7 days, respectively.

The preceding experiments were performed in light for 12 min or in the dark every day. Experiments were repeated three times.

1.14. Measurement of antimicrobial activity. Staphylococcus aureus (*S. aureus*) and Escherichia coli (*E. coli*) were introduced into the lysate medium respectively and incubated at 37 ℃ in a shaker. After overnight cultures, *S. aureus* or *E. coli* were diluted to OD600 = 0.5, and 80 ug mL^{-1} EDTA-CDs and Fe@EDTA-CDs were prepared in 0.9% NaCl solution, respectively. The bacterial suspension was mixed with different concentrations of EDTA-CDs and Fe@EDTA-CDs solutions, followed by the addition of 100 uM of H_2O_2, and then diluted 10^4 times with nutrient broth after xenon light irradiation. The diluted bacterial solution was spread on an agar plate, irradiated with an LED light for 10 minutes, and the number of bacterial colonies was counted after incubation at 37 ℃ for 24 h.

2. Figures S1-S22 and Tables S1-S3

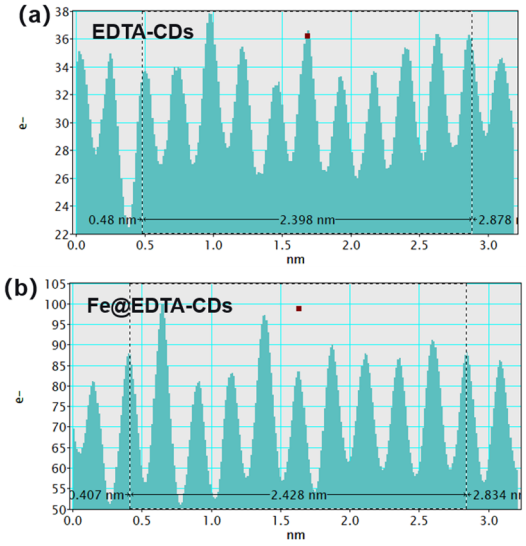

Figure S1. Line profile of diffraction fringes for the (a) EDTA-CDs and (b) Fe@EDTA-CDs.

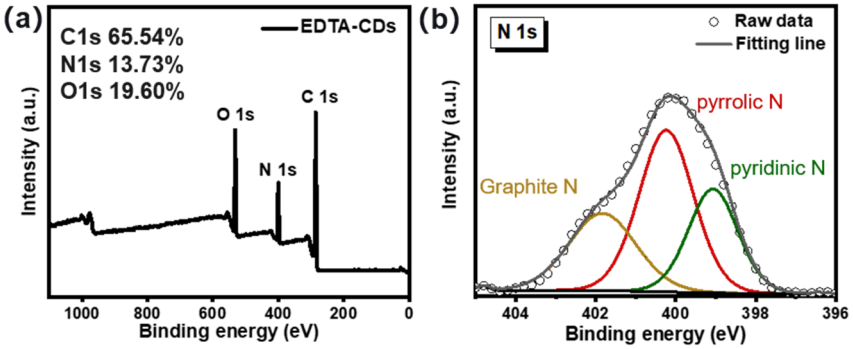

Figure S2. (a) XPS survey and (b) High-resolution N 1s spectra of EDTA-CDs.

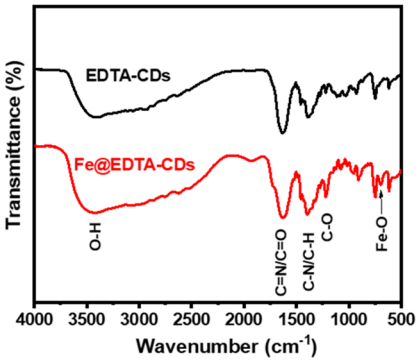

Figure S3. FT-IR spectra of EDTA-CDs and Fe@EDTA-CDs.

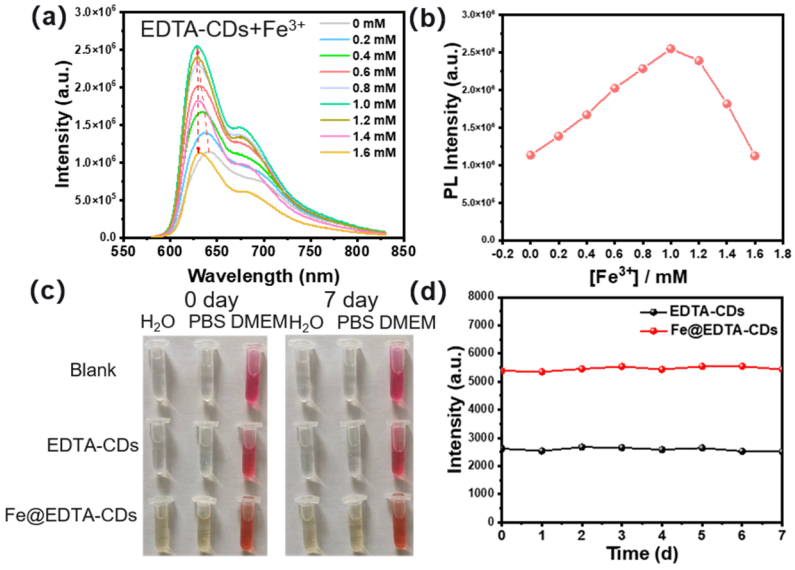

Figure S4. (a) PL spectra and (b) PL intensity changes of maximum emission of 1 mg mL^{-1} EDTA-CDs in aqueous medium with different concentrations of Fe^{3+} (from 0 to 1.6 mM). (c) The dispersed stability of the EDTA-CDs and Fe@EDTA-CDs in various physiological media. (d) PL intensity of the EDTA-CDs and Fe@EDTA-CDs in different periods.

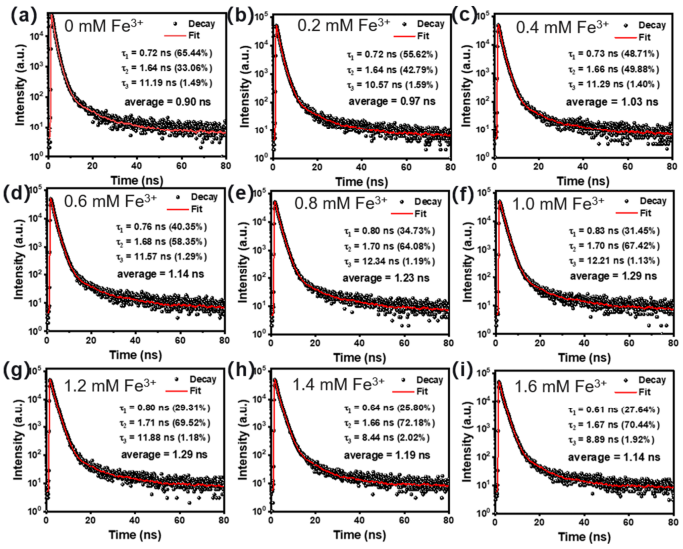

Figure S5. Fluorescence decay curves of EDTA-CDs in an aqueous medium with different concentrations of Fe^{3+} (from 0 to 1.6 mM) at 505 nm.

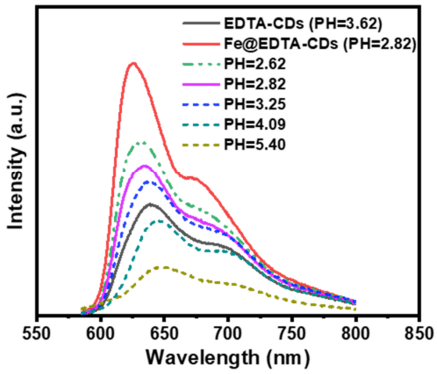

Figure S6. PL spectra (λ_{ex} = 570 nm) of EDTA-CDs, Fe@EDTA-CDs and EDTA-CDs in different pH solutions.

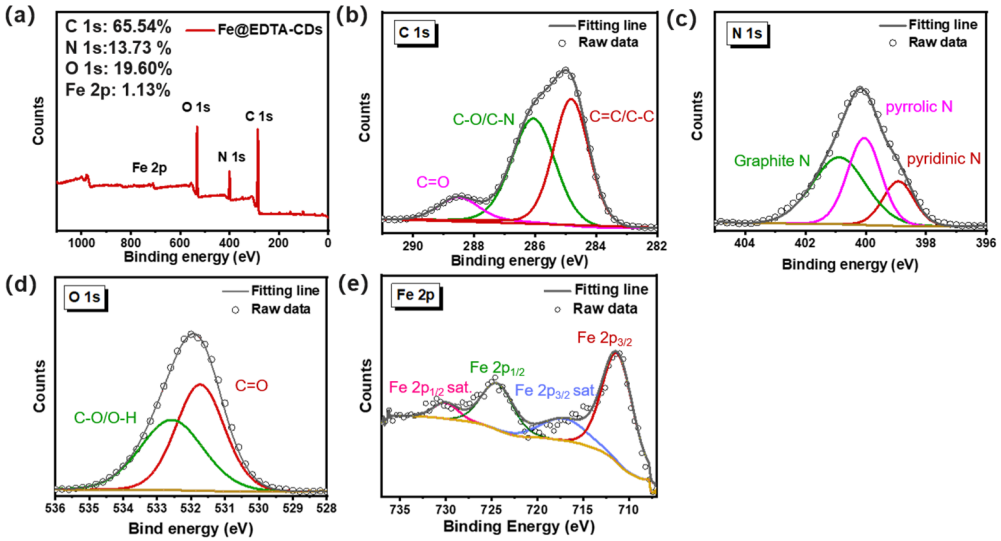

Figure S7. (a) XPS survey spectra of Fe@EDTA-CDs. High-resolution C 1s (b), N 1s (c), O 1s (d) and Fe $2p_{1/2}$, Fe $2p_{3/2}$ (e) spectra of Fe@EDTA-CDs.

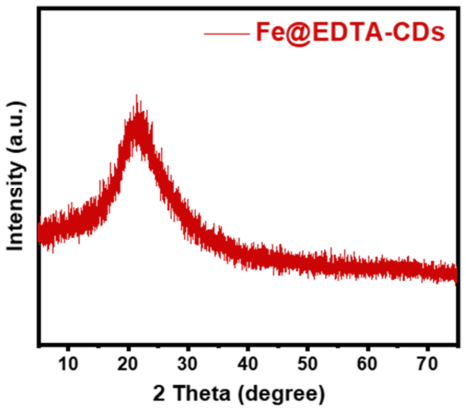

Figure S8. XRD pattern of Fe@EDTA-CDs.

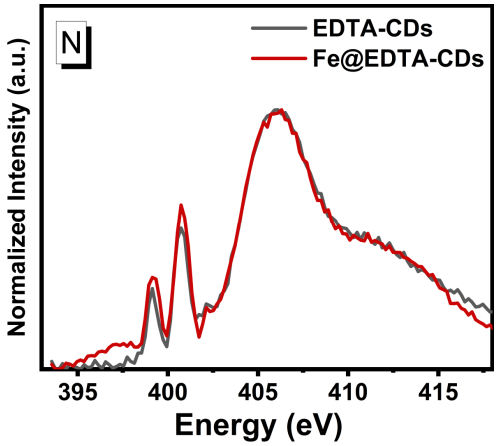

Figure S9. N K-edge XANES spectra of EDTA-CDs and Fe@EDTA-CDs.

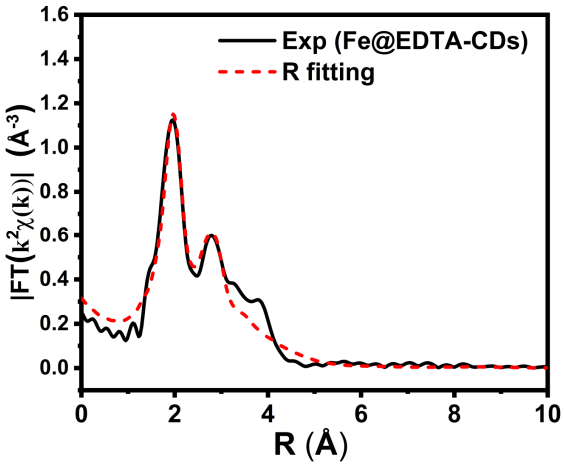

Figure S10. The corresponding EXAFS fitting curve of Fe@EDTA-CDs at *R* space.

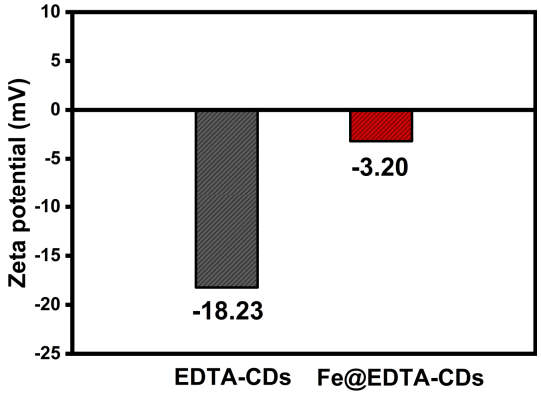

Figure S11. Zeta potentials of EDTA-CDs and Fe@EDTA-CDs.

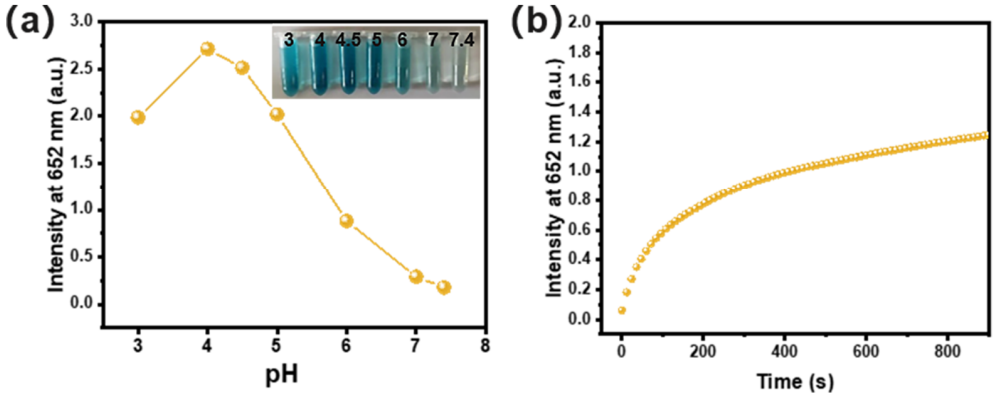

Figure S12. (a) pH (the inset is the corresponding photographs) and (b) time-dependent absorbance changes at 652 nm.

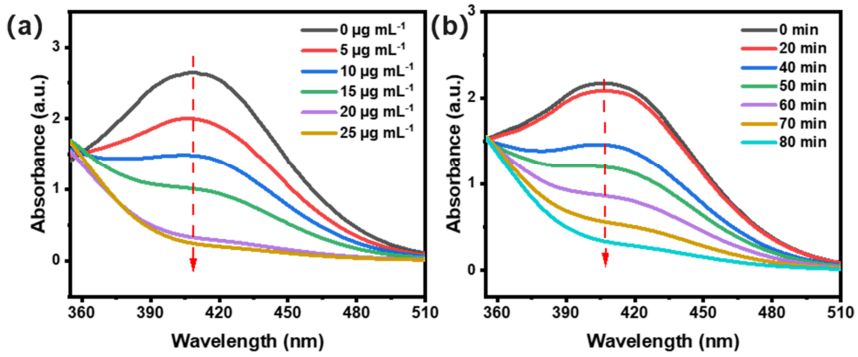

Figure S13. (a) GSH depletion with different concentrations of Fe@EDTA-CDs presented by measuring the absorbance of DTNB after 80 min reaction (GSH: 1mM) (b) GSH depletion by Fe@EDTA-CDs (GSH: 1 mM and Fe@EDTA-CDs: 20 μg mL^{-1}).

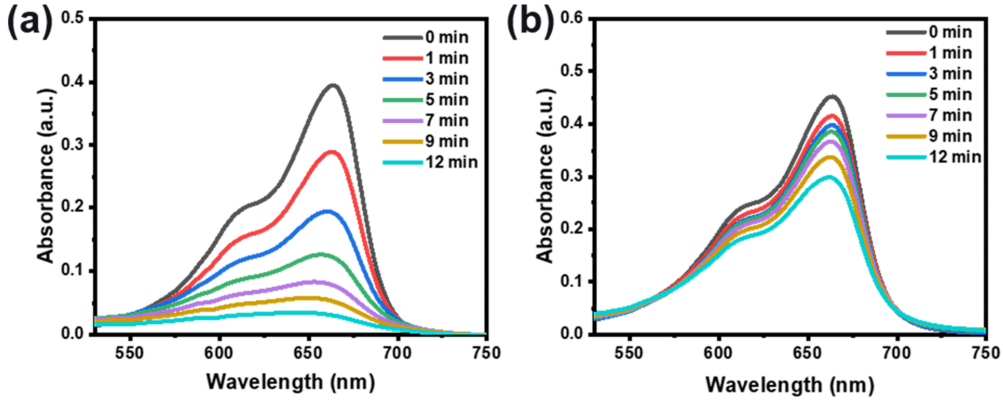

Figure S14. Time-dependent degradation of MB after adding (a) Fe@EDTA-CDs/H_2O_2 and (b) EDTA-CDs/H_2O_2 under visible light irradiation (LED lamp, 400-500 nm, 100 mW cm^{-2}).

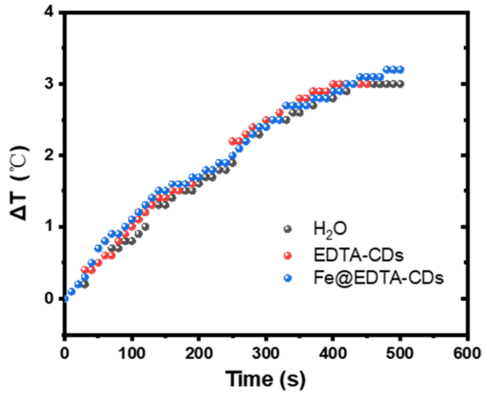

Figure S15. Photothermal temperature rise of water, EDTA-CDs and Fe@EDTA-CDs in aqueous solution under visible light irradiation (LED lamp, 400-500 nm, 100 mW cm^{-2}).

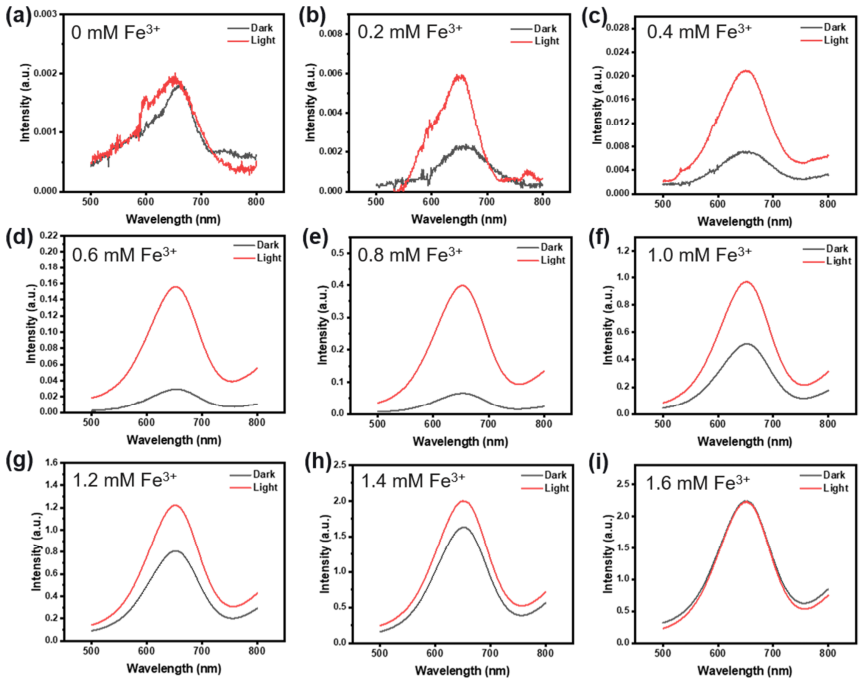

Figure S16. Under the addition of different Fe^{3+} concentrations, visible light irradiation for 2 minutes (LED lamp, 400-500 nm, 100 mW cm^{-2}), increased oxTMB absorbance changes.

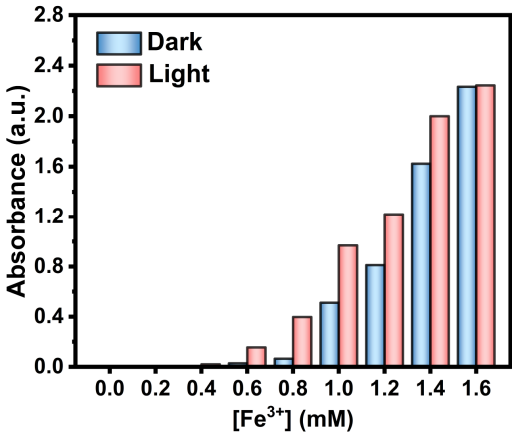

Figure S17. The absorbance value of oxTMB at 652nm corresponding to different Fe^{3+} concentrations under the condition with or without visible light irradiation (LED lamp, 400-500 nm, 100 mW cm^{-2}).

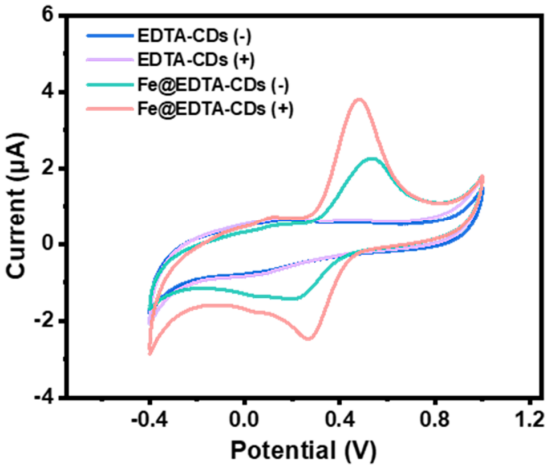

Figure S18. CV curves of Fe@EDTA-CDs/glassy carbon electrode and EDTA-CDs/glassy carbon electrode in acetate buffer solution (0.1 M, pH = 4) in presence (+) and absence (-) of visible light irradiation (LED lamp, 400-500 nm, 100 mW cm^{-2})

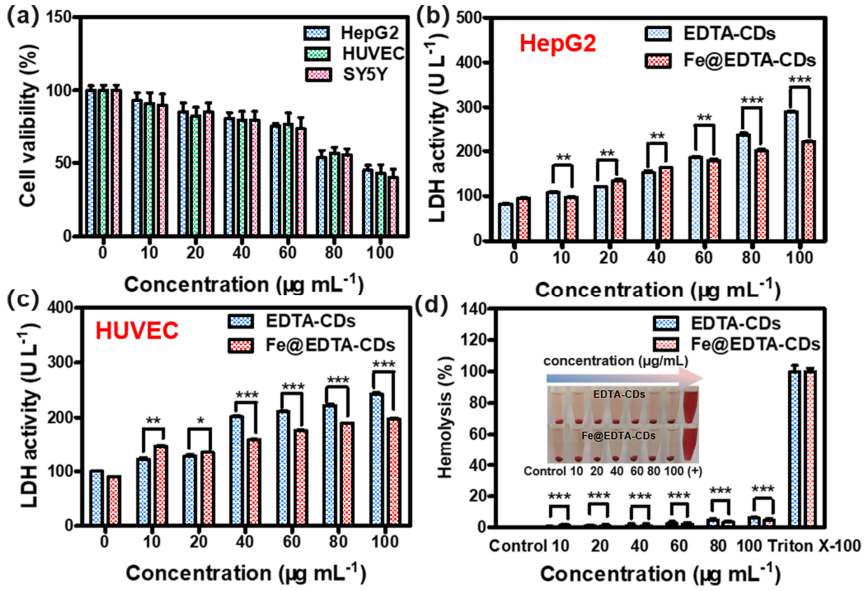

Figure S19. (a) Cell viability of different cells incubated with EDTA-CDs at different concentrations. LDH release from the HepG2 cells (b) and HUVEC cells (c) treated with the EDTA-CDs and Fe@EDTA-CDs for 24 h at increasing concentrations. (d) Hematological evaluation of RBCs treated with different dosages of EDTA-CDs and Fe@EDTA-CDs, the insets are the corresponding photographs.

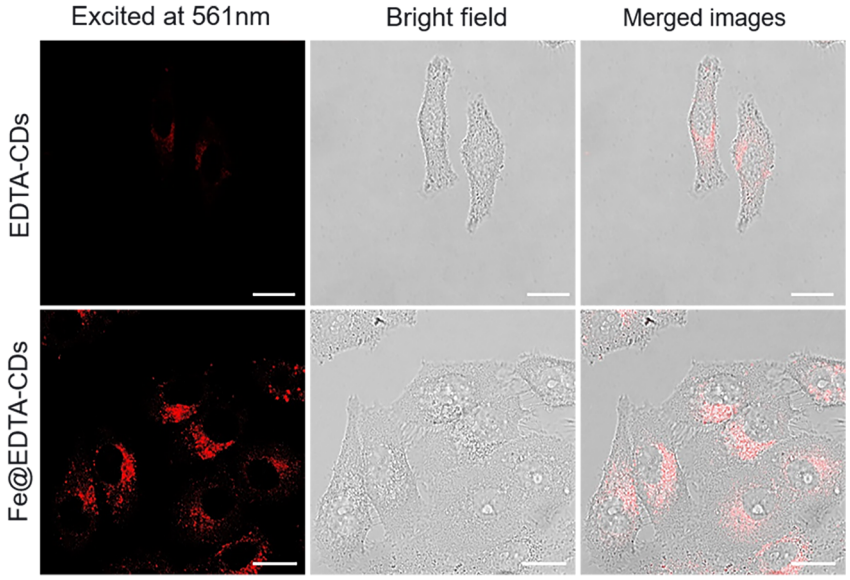

Figure S20. CLSM images of HepG2 cells incubated with 80 μg mL^{-1} EDTA-CDs and Fe@EDTA-CDs. Scale bar: 20 μm.

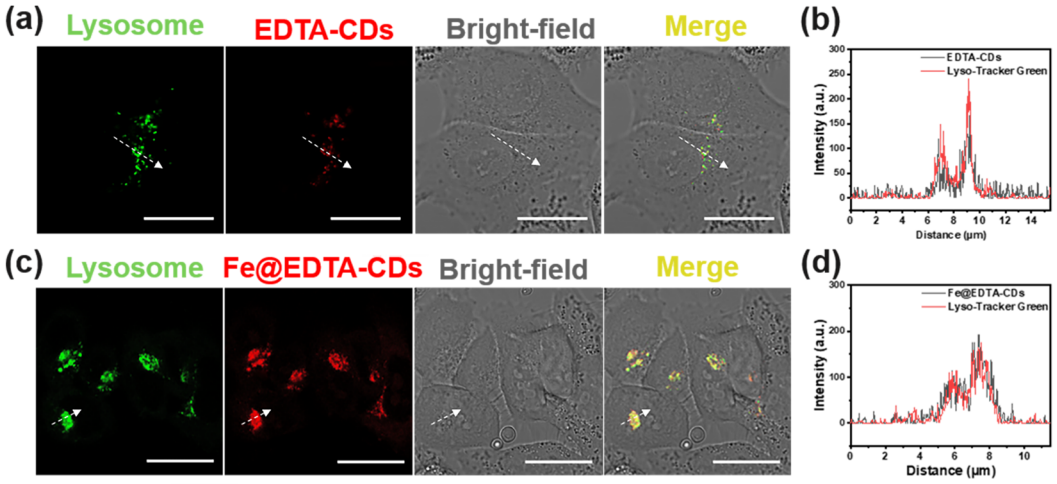

Figure S21. (a) CLSM images of HepG2 cells incubated with 80 μg mL^{-1} EDTA-CDs and 100 nM Lyso-Tracker Green. Scale bar: 20 μm. (b) The fluorescence intensity curve between the green and red channels in HepG2 cells. (c) CLSM images of HepG2 cells incubated with 80 μg mL^{-1} Fe@EDTA-CDs and 100 nM Lyso-Tracker Green. Scale bar: 20 μm. (d) The fluorescence intensity curve between the green and red channels in HepG2 cells.

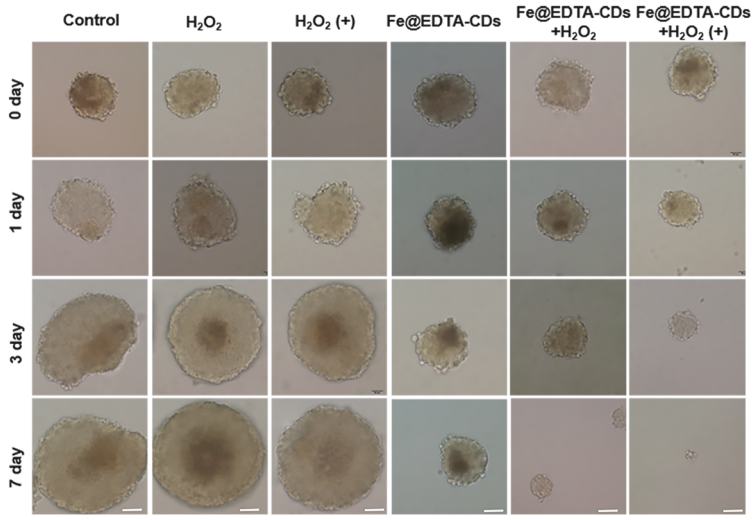

Figure S22. Images of SY5Y 3D MCs co-incubated with medium, H_2O_2, Fe@EDTA-CDs+H_2O_2 These images were captured daily under darkness or visible light irradiation (12 min, 400-500 nm, 100 mW cm^{-2}). Scale bar = 100 μm.

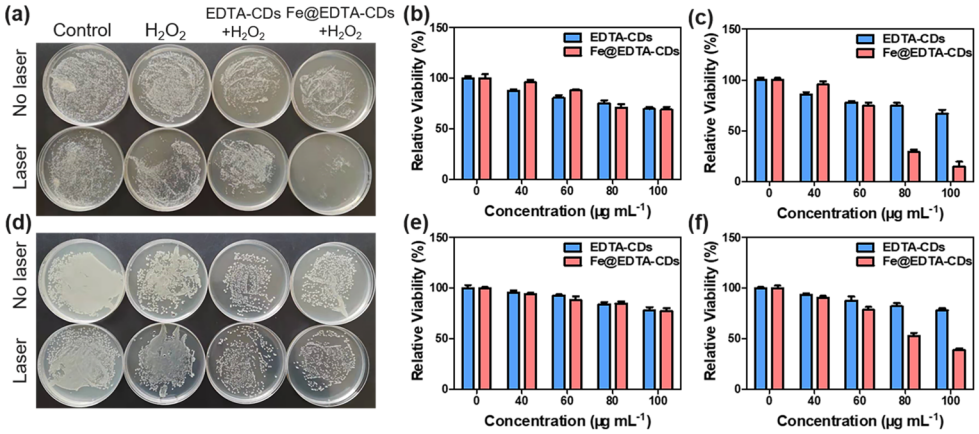

Figure S23. Agar plate photographs of the control, H_2O_2 (100 μM), EDTA-CDs (80 μg mL^{-1}) + H_2O_2 and Fe@EDTA-CDs (80 μg mL^{-1}) + H_2O_2 against *S. aureus* (a) and *E. coli* (d). The antibacterial activities against *S. aureus* under (b) no illumination, (c) LED lamp illumination for 10 min. The antibacterial activities against *E. coli* under (e) no illumination, (f) xenon lamp illumination for 10 min.

Table S1. Structural parameters extracted from the Fe K-edge χ(R) space spectra fitting of Fe@EDTA-CDs.

Fe@EDTA-CDs	amp/ S_0^2	N (Fe-O path)	R (Fe-O path) (Å)	σ^2 (Fe-O path) (10^{-3}Å^2)	ΔE_0 (eV)
	0.95+/-0.16	4	2.006± 0.087	2.2+/-0.8	1.56+/-0.94
	amp/ S_0^2	N (Fe-O-C path)	R (Fe-O-C path) (Å)	σ^2 (Fe-O-C path) (10^{-3}Å^2)	ΔE_0 (eV)
	1.14+/-0.12	4	2.953± 0.102	4.5+/-1.4	3.46+/-1.02

Table S2. The catalytic kinetic parameters of Fe@EDTA-CDs, Fe_3O_4, and HRP.[S1]

Catalyst	Substrate	K_m (mM)	v_{max} (μM s^{-1})
Fe@EDTA-CDs	H_2O_2	1.47	0.663
Fe_3O_4	H_2O_2	154	0.0978
HRP	H_2O_2	3.70	0.0871

Table S3. Comparison of the catalytic kinetic constants of Fe@EDTA-CDs to H_2O_2 and other reported artificial enzymes.

Artificial enzymes	K_m (mM)	v_{max} (μM s^{-1})	TON (10^{-3} s^{-1})	Ref.
Fe@EDTA-CDs	1.47	0.663	38.7	This work
MnO_2	/	0.006	0.056	[S2]
Mn_2O_3	12.530	1.010	7.979	[S2]
Mn_3O_4	/	0.013	0.099	[S2]
CoO	92.100	1.140	8.550	[S2]
CeO_2	4.410	0.180	3.096	[S2]
Fe_3O_4	41.660	0.160	1.237	[S2]
CuO	31.180	0.280	2.240	[S2]
Co_3O_4	41.750	0.260	2.087	[S2]
NiO	/	0.011	0.821	[S2]
Fe-N-C	0.012	0.223	36.700	[S3]
Fe-N-C SAzyme	4.310	0.620	3.990	[S4]
Cu NPs/N-C	17.980	0.060	3.300	[S3]
Fe-MOF	0.0013	0.025	0.510	[S5]
PtFe@Fe_3O_4	53.550	0.108	8.617	[S6]
PtFe	217.600	0.082	2.200	[S6]
Pt hollow	6.900	0.099	14.140	[S7]

References

[S1] L. Gao, J. Zhuang, L. Nie, J. Zhang, Y. Zhang, N. Gu, T. Wang, J. Feng, D. Yang, S. Perrett, X. Yan, *Nat. Nanotechnol*. **2007**, *2*, 577.

[S2] X. Wang, X. Gao, L. Qin, C. Wang, L. Song, Y. Zhou, G. Zhu, W. Cao, S. Lin,

L. Zhou, K. Wang, H. Zhang, Z. Jin, P. Wang, X. Gao, H. Wei, *Nat. Commun*. **2019**, *10*, 704.

[S3] Y. Wu, J. Wu, L. Jiao, W. Xu, H. Wang, X. Wei, W. Gu, G. Ren, N. Zhang, Q. Zhang, L. Huang, L. Gu, C. Zhu, *Anal. Chem*. **2020**, *92*, 3373.

[S4] L. Jiao, J. Wu, H. Zhong, Y. Zhang, W. Xu, Y. Wu, Y. Chen, H. Yan, Q. Zhang, W. Gu, L. Gu, S. Beckman, L. Huang, C. Zhu, *ACS Catal*. **2020**, *10*, 6422.

[S5] W. Xu, L. Jiao, H. Yan, Y. Wu, L. Chen, W. Gu, D. Du, Y. Lin, C. Zhu, *ACS Appl. Mater. Interfaces* **2019**, *11*, 22096.

[S6] S. Li, L. Shang, B. Xu, S. Wang, K. Gu, Q. Wu, Y. Sun, Q. Zhang, H. Yang, F. Zhang, L. Gu, T. Zhang, H. Liu, *Angew. Chem. Int. Ed*. **2019**, *58*, 12624.

[S7] R. Wu, Y. Chong, G. Fang, X. Jiang, Y. Pan, C. Chen, J. Yin, C. Ge, *Adv. Funct. Mater*. **2018**, *28*, 1801484.